ACS NANO

www.acsnano.org

PERSPECTIVE

Endosomal Escape of Lipid Nanoparticles: A Perspective on the Literature Data

Dehua Pei*

Cite This: *ACS Nano* 2025, 19, 40293−40303

Read Online

ACCESS | Metrics & More | Article Recommendations

ABSTRACT: **Endosomal escape remains a critical bottleneck for the intracellular delivery of nucleic acids by lipid nanoparticles (LNPs), largely due to its low efficiency and poorly understood mechanism. While various models, including proton sponge effect/osmotic lysis and membrane destabilization/fusion, have been proposed, none are fully validated or sufficient for guiding rational LNP design. Herein, I reevaluate existing data, presenting strong evidence that LNPs escape the endosomal compartment through the recently discovered vesicle budding-and-collapse (VBC) mechanism. A critical subsequent finding is that endosomal escape triggers the formation of an insoluble lipid/nucleic acid aggregate within the cytoplasm. The slow dissolution of this aggregate emerges as an additional, potentially rate-limiting, bottleneck to functional nucleic acid delivery. By reconciling previously puzzling experimental observations, the VBC mechanism provides a powerful theoretical framework for the rational design of LNPs with enhanced endosomal escape and overall functional delivery efficiencies.**

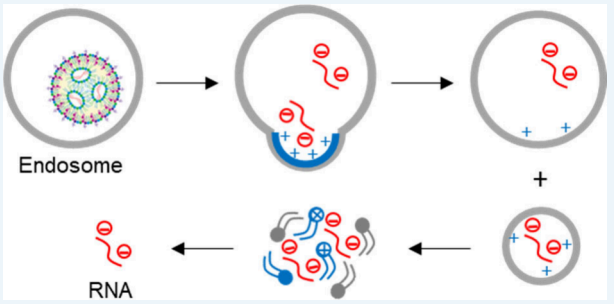

KEYWORDS: *drug delivery, endosomal escape, lipid nanoparticle, membrane transport, vesicle budding and collapse*

INTRODUCTION

Lipid nanoparticles (LNPs) have revolutionized nucleic acid delivery, establishing themselves as a powerful platform for encapsulating and transporting fragile genetic payloads.[1,2] This capability has profoundly transformed our approach to treating a vast array of diseases, including those previously considered "undruggable" by small molecules or conventional biologics. Landmark examples include the development of Onpattro (patisiran), the first FDA-approved small interfering RNA (siRNA) therapeutic for hereditary transthyretin-mediated amyloidosis,[3] and the rapid deployment of mRNA vaccines during the COVID-19 pandemic.[4] Despite these successes, the full therapeutic potential of LNPs remains largely unrealized. Their journey from the bloodstream to the cytosol of target cells is fraught with challenges, notably inadequate biodistribution into extrahepatic tissues[5] and, critically, extremely low cytosolic delivery efficiency.[6,7]

LNPs are internalized by eukaryotic cells through a combination of various endocytic pathways, including receptor-mediated endocytosis, macropinocytosis, and phagocytosis.[8] When introduced into the bloodstream, LNPs are quickly coated with proteins, notably apolipoprotein E (ApoE), which facilitates cellular uptake by recognizing and binding to the LDL receptor on the cell surface. Regardless of the uptake mechanism, the internalized LNPs are initially entrapped within the early endosomes.[9,10] From this point, they are either recycled back to the cell surface[10] or advance through a progressively acidic environment and face a barrage of degradative enzymes as early endosomes mature into late endosomes and ultimately fuse with lysosomes. To exert their therapeutic effect, the encapsulated nucleic acid cargo—whether mRNA, siRNA, or other genetic material—must successfully escape this degradative "endosomal labyrinth" and reach the cytoplasm, the essential site for protein synthesis and gene regulation. This process of endosomal escape is widely acknowledged as the primary bottleneck in LNP-mediated drug delivery,[6,7] with a dismal 1−3% of internalized siRNA or mRNA typically reaching the cytosol.[9,11,12] Compounding this challenge, the precise molecular mechanism of LNP endosomal escape remains poorly understood, despite decades of intensive research.[6] Existing mechanistic models, such as the proton sponge effect/osmotic lysis[13] and membrane destabilization/fusion mechanisms,[14] lack comprehensive experimental vali-

Received: July 12, 2025
Revised: November 13, 2025
Accepted: November 14, 2025
Published: November 20, 2025

dation and have proven insufficient to guide the rational design of more efficient LNPs. Consequently, researchers have largely relied on empirical methods, such as library screening, to discover LNPs with incrementally improved performance.

The past decade or so has witnessed two pivotal advancements that offer new perspectives on biomolecule membrane translocation. First, we discovered a novel membrane translocation mechanism, vesicle budding and collapse (VBC).[15−18] We demonstrated that cell-penetrating peptides (CPPs)[15,16] and bacterial protein toxins[17] employ the VBC mechanism to escape endosomes and later found that CPPs can also directly translocate across the plasma membrane of mammalian cells via VBC.[18] Further, a survey of the literature suggests that VBC may represent a fundamental, unifying mechanism for the membrane transport of diverse biomolecules (e.g., peptides and proteins) and molecular assemblies (e.g., polyplexes and nonenveloped viruses).[19,20] Second, significant advancements in live-cell imaging techniques have enabled real-time, high-resolution monitoring of LNP endocytic uptake and intracellular trafficking.[21,22] As will be detailed below, these studies have confirmed the ability of LNPs to breach the endosomal membrane and deliver nucleic acid payloads into the cytosol, generating a wealth of experimental data. However, a cohesive mechanistic interpretation that integrates these observations has been conspicuously absent.

This *Perspective* aims to address this critical gap by delving into the intricate interactions between LNPs and the endosomal membrane. I will begin by critically reviewing previous mechanistic models of LNP endosomal escape, highlighting their strengths and inherent limitations. Subsequently, I will introduce the VBC mechanism, present compelling evidence suggesting that LNPs escape the endosome primarily through the newly elucidated VBC mechanism, and demonstrate its capacity to reconcile key, previously enigmatic experimental data reported in the literature. Finally, I will discuss key mechanistic studies that need to be completed in the future and the profound implications of the VBC mechanism for guiding future LNP design, ultimately enhancing their therapeutic efficacy.

PREVIOUS MODELS OF LNP ENDOSOMAL ESCAPE

LNPs are precisely engineered formulations comprising a blend of cationic ionizable lipids (CILs), phospholipids, cholesterol, and PEGylated lipids.[1,2] CILs are pivotal to LNP function; largely neutral at physiological pH, they become positively charged within the acidic endosomal environment. This pH-dependent charging is crucial not only for binding, condensing, and encapsulating negatively charged nucleic acid payloads during LNP assembly, but also for facilitating their subsequent release into the cytoplasm. Traditionally, two prominent models, proton sponge effect/osmotic lysis[13] and membrane destabilization/fusion,[14] have been invoked to explain LNP endosomal escape, both hinging on the physicochemical consequences of CIL protonation.

The proton sponge/osmotic lysis model was originally proposed in the 1990s to explain the high efficiency of polycations like polyethylenimine (PEI) in delivering nucleic acids.[13] It posits that the amine groups of PEI become highly protonated in the acidic endosomal environment, acting as a ″proton sponge″ that absorbs protons pumped into the endosome by the V-ATPase, buffering endosomal pH and impeding acidification. This buffering drives a continuous influx of protons into the endosome as the cell attempts to restore its pH. To neutralize the accumulating positive charge, chloride ions are cotransported, increasing osmotic pressure within the endosome. This osmotic imbalance leads to water influx, causing the endosome to swell and eventually rupture, thereby releasing the nucleic acid cargo into the cytoplasm. This model became popular with LNPs because it provided a simple and plausible explanation for several experimental observations: the strict requirement for endosomal acidification,[23−26] the sudden release of nucleic acid cargo into the cytosol (or "quantal" kinetics),[11,27−30] and the fact that efficacious CILs typically have a pK_a of approximately 6.4.[14,26] That latter is similar to the pH of early/maturing endosomes (pH 6.0−6.5), the primary site of LNP escape. However, the proton sponge hypothesis faces significant challenges. Many compounds, including some ionizable lipids with pK_a values around 6.4,[26] fail to induce endosomal escape. Conversely, biomolecules/ions like CPP12[15,16] and Ca^{2+},[31] which do not undergo protonation during endosomal acidification, can nonetheless trigger robust endosomal escape, indicating that protonation of the translocating species is neither necessary nor sufficient for this process. Furthermore, PEGylation of cationic polymers or lipids, while not altering their pK_a, is well-known to reduce the endosomal escape efficiency of polyplexes and liposomes.[32,33]

In the membrane destabilization/fusion model, protonated CILs directly interact with the negatively charged lipids of the endosomal membrane.[14] The resulting inverse cone-shaped CIL/phospholipid pairs induce negative membrane curvature and a transition from lamellar to nonlamellar phases (often to an inverse hexagonal H_{II} phase).[34,35] This phase change causes the LNP and endosomal membranes to fuse or create transient pores in the endosomal membrane, releasing the cargo. This model for LNPs gained popularity due to a strong correlation between the acidic pH of the endosome and the physicochemical properties of the CILs.[14,26] Key evidence included: 1) Structure−activity relationship (SAR) studies showed that LNP efficacy peaks when the CIL's pK_a is in the endosomal pH range, confirming protonation as the escape trigger.[14,26] 2) Biophysical studies demonstrated that, at low pH, the protonated lipids switch from a stable lamellar configuration to a highly disruptive nonlamellar phase (the H_{II} phase).[14,36] This phase transition, linked to the molecular shape change of the lipid and the concept of a negative molecular packing parameter, promotes direct membrane fusion and destabilization, offering a potential physical explanation for LNP efficacy. However, recent live-cell imaging studies revealed striking similarities in the endosomal escape of polyplexes, lipoplexes, and LNPs, e.g., they all cause *sudden but incomplete* release of free nucleic acid cargo from damaged endosomes.[11,27−30] Polyplexes, being noncovalent complexes of cationic polymers and nucleic acids, cannot fuse with the endosomal membrane. Membrane fusion would lead to the complete release of nucleic acid cargo, while formation of transient pores would lead to the sequential, rather than sudden, release of cargo. Furthermore, endosomal escape has been demonstrated for very large biomolecules, e.g., Cas9 mRNA;[37] with a molecular weight of 1.46 MDa and a hydrodynamic radius of 15−20 nm, the endosomal escape of Cas9 mRNA would necessitate a pore size of at least 20 nm in the endosomal membrane. It is difficult to comprehend how the Cas9 mRNA might be released through such a pore without also losing most of the other endosomal contents.

https://doi.org/10.1021/acsnano.5c11721
ACS Nano 2025, 19, 40293−40303

ENDOSOMAL ESCAPE VIA THE VBC MECHANISM

Membrane translocation via the VBC mechanism generally proceeds through a series of defined steps (Figure 1).[15−20]

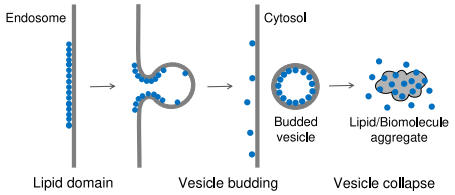

Figure 1. Schematic representation of the translocation of biomolecules (blue spheres) across a cell membrane (gray line) via the VBC mechanism.

Initially, the biomolecule of interest binds to the target membrane (e.g., an endosomal membrane) through electrostatic and/or hydrophobic interactions. Multidentate interactions between the biomolecules and membrane phospholipids—for instance, an arginine side chain of the biomolecule can simultaneously interact with the phosphate head groups of two phospholipids—induce phospholipid clustering and concomitant oligomerization of the biomolecules. This process results in the formation of a distinct lipid domain enriched in the biomolecules. Driven by membrane curvature induced by these biomolecules and/or line tension between this lipid domain and the surrounding membrane, the domain then buds outward, forming a small vesicle that encapsulates the biomolecules. Following its formation, this nascent vesicle, being highly curved and inherently unstable, rapidly disintegrates or collapses, releasing its contents into the new cellular compartment, such as the cytosol.

The VBC mechanism is fundamentally distinct from all other known membrane transport mechanisms, due to its several unique features/properties. First, biomolecules translocate a cell membrane *topologically*—moving from one side of the membrane to the other—but do not *physically* pass through the lipid bilayer. As such, the VBC mechanism is agnostic to the chemical nature (peptide, protein, lipid, or small molecule) or size of the active agent, so long as it can induce the necessary membrane curvature and budding. Second, translocation of biomolecules, either small or large, does not compromise the structure of the biomolecules (e.g., protein unfolding or dissociation of a noncovalent complex) or the barrier function of the cell membrane. Third, each VBC event facilitates the transfer of a small volume of the donor compartment into the receiving compartment, thus passively transporting any molecules and ions contained within that volume, even if not directly associated with the translocating biomolecule (e.g., the endosomal escape of CPPs releases 10-kD dextran into the cytosol[16]).

The VBC mechanism was initially discovered during our investigations into the endosomal escape of CPPs.[15,16] Subsequently, we found that large, folded proteins, such as Diphtheria toxin (DT) and NleC, also utilize the VBC pathway for endosomal escape.[17] Emerging evidence suggests that VBC may be employed by a broad spectrum of biomolecules, including peptides, folded proteins, nonenveloped viruses, and synthetic drug delivery vehicles such as polyplexes, lipoplexes, and LNPs.[19,20] For the endosomal escape of LNPs via VBC, I propose the following sequence of events shown in Figure 2.

LNP Entry and Disintegration. LNPs, carrying their nucleic acid cargo, enter cells via multiple endocytosis pathways and are initially trapped within early endosomes. As the endosomes mature and acidify, the CILs within the LNP become protonated. This protonation leads to destabilization of the LNP structure and the release of its components, including CILs, helper lipids, and the RNA cargo.

Cationic Lipid Domain Formation and RNA Colocalization. The released CILs and helper lipids, driven by their hydrophobicity, insert into the inner leaflet of the endosomal membrane. Rather than dispersing uniformly, the CILs self-assemble into distinct, enriched domains. This domain formation is likely influenced by the unique, inverse cone-

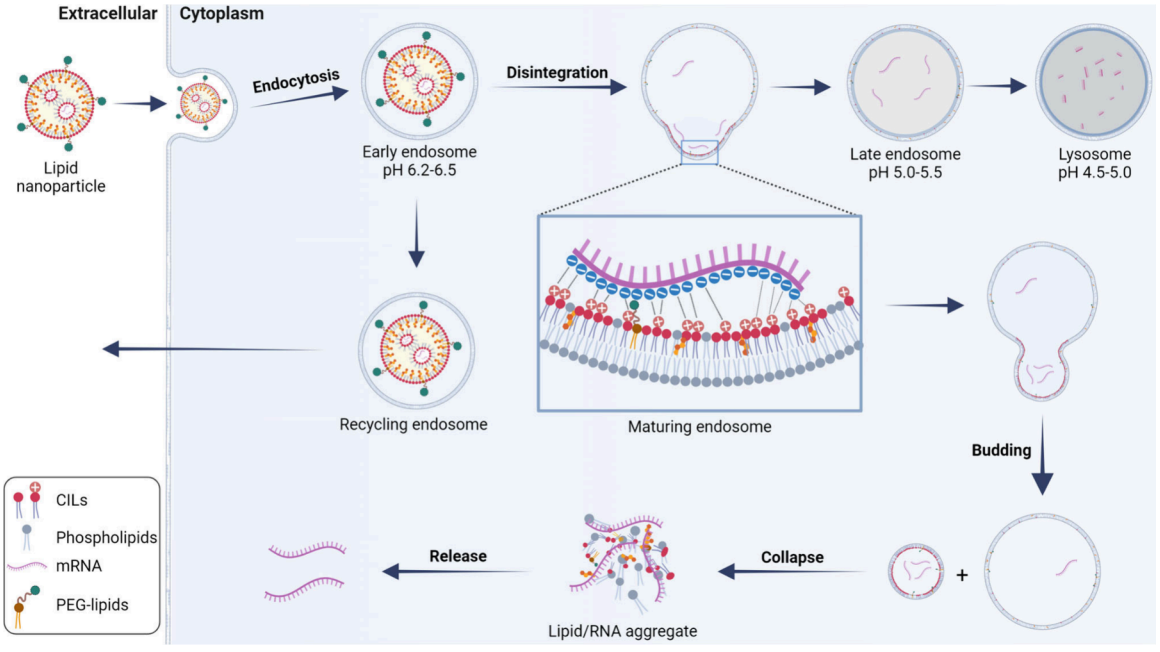

Figure 2. Proposed mechanism for the endosomal escape of LNPs. Created in BioRender by Bhat, P. (2025).

https://doi.org/10.1021/acsnano.5c11721
ACS Nano 2025, 19, 40293−40303

shaped structures of CILs, which interact suboptimally with the inherent phospholipids of the endosomal membrane. Simultaneously, the negatively charged RNA molecules are drawn to these growing cationic lipid domains through strong electrostatic interactions.

Vesicle Budding and Collapse. The inverse cone-shaped CILs generate negative membrane curvature within the lipid domain, which invaginates to form a small vesicle, potentially aided by specific cellular membrane-remodeling proteins including small GTPases, adaptor and coat proteins, ESCRT complexes, SNARE proteins, and the cytoskeleton. RNA molecules electrostatically attracted to the CIL domain are recruited and encapsulated into the vesicle. The nascent vesicle is inherently unstable, likely due to its high membrane curvature and high concentrations of CILs, causing it to spontaneously collapse. This collapse yields an amorphous aggregate of lipids, nucleic acids, and potentially cellular proteins within the cytoplasm.

Cargo Release. The kinetics of cargo dissolution from this aggregate and subsequent liberation into the cytoplasm may vary significantly depending on the nature of the lipids and the nucleic acid cargo. It is anticipated that smaller cargos (e.g., siRNA) are more readily (at least partially) released, whereas larger cargos (e.g., mRNA) may present a greater challenge, constituting another bottleneck for efficient nucleic acid delivery. This is because larger molecules inherently have more points of contact (hundreds/thousands of negative charges on mRNA vs 42 on siRNA) with the highly positively charged lipid domains, leading to greater binding affinity. Similarly, CILs that pack tightly against each other likely form more stable aggregates, slowing the release of nucleic acid cargo.

Since free CILs (and likely other components) released from disassembled LNPs drive VBC/endosomal escape, the above sequence of events is expected to be conserved for all LNPs, regardless of their initial structure or the endocytic entry route.

LITERATURE DATA SUPPORT THE VBC MECHANISM

To the best of our knowledge, the proposed VBC mechanism is fully consistent with the current literature's key observations and offers a superior mechanistic explanation for the experimental data. The following sections detail key experimental evidence supporting each step of the VBC mechanism.

LNP Entry and Disintegration. Acidic pH-induced LNP disassembly has been observed in live cells and effectively recapitulated in model systems. Sahay et al. quantitatively assessed LNP disassembly kinetics in HeLa cells using a fluorescence resonance energy transfer (FRET) assay.[10] They loaded LNPs with two identical siRNAs, each labeled with a different fluorophore forming a FRET pair. The close packing of siRNA within intact LNPs generates a FRET signal, which diminishes upon LNP disassembly. Flow cytometry of HeLa cells treated with these LNPs revealed a time-dependent decrease in the FRET signal within one hour of internalization, while the fluorescence from a single fluorophore (AF647) remained constant. Nanoparticle disassembly was largely complete after one hour, with free siRNAs remaining trapped inside endosomes. After 24 h, a significant fraction (70%) of the siRNAs was recycled out of the cells.

Wittrup and colleagues employed super-resolution Airyscan microscopy to image HeLa cells incubated with AF647-labeled siRNA-LNPs and Cy5-labeled mRNA-LNPs.[30] They observed apparently intact LNPs within the lumen of $EEA1^+$ early endosomes, but generally homogenously dispersed siRNA signals filling the entire lumen of $CD63^+$ late endosomes. For mRNA-LNPs, the mRNA payload was typically more dispersed in $CD63^+$ vesicles than in $EEA1^+$ endosomes, though partly condensed mRNA-LNP remnants were still visible in $CD63^+$ vesicles. In $Rab5^+$ endosomes, siRNA-LNPs displayed a wide range of structures, from largely intact LNPs to vesicles with homogeneous siRNA distribution. These observations collectively indicate that LNPs begin to disintegrate within early/maturing endosomes—the typical site of endosomal escape—and are largely disassembled by the time they reach late endosomes.

Other researchers have utilized model membranes to further investigate LNP disassembly and the subsequent membrane insertion of CILs. Spadea et al. used Langmuir monolayers to study LNP interactions with model early and late endosomal membranes as a function of pH and RNA cargo type.[38] Physicochemical insights were derived by comparing surface pressure (a measure of lipid density) with optical phase shift from ellipsometry and interfacial morphology from Brewster angle microscopy (BAM) imaging. At pH 6.5 and 5.5, LNP addition induced a rapid increase in surface pressure following a variable lag period, consistent with the abrupt collapse of LNP structure and subsequent insertion of LNP-derived CILs into the model membrane. At pH $\geq$ 7, lipid insertion was minimal, and LNPs bound to the monolayer surface as intact nanoparticles.

Aliakbarinodehi et al. employed surface-sensitive fluorescence microscopy with single LNP resolution to examine pH-controlled interactions between individual LNPs and a planar anionic supported lipid bilayer (SLB), mimicking the electrostatic conditions of the early endosomal membrane.[39,40] A sharp increase in LNP binding was observed when the pH was lowered from 6.6 to 6.0, accompanied by stepwise, large-scale LNP disintegration. Similar to the findings of Spadea et al., a delay in the onset of LNP binding was observed after the pH drop. Upon LNP binding and disintegration, a significant fraction (~70%) of mRNA was rapidly released into the acidic solution, representing the endosomal lumen; over time, some of the released mRNA rebound to the SLB. Rapid insertion of the released LNP lipids into the surrounding areas of the SLB was also observed. Interestingly, a fraction (~30%) of mRNA remained bound to the SLB even after the pH was reverted to neutral cytosolic conditions.

Cationic Lipid Domain Formation and RNA Colocalization. The formation of lipid domains enriched in the translocating biomolecule is a prerequisite for membrane translocation via the VBC mechanism.[18,41,42] However, direct visualization of these lipid domains on endosomal membranes is challenging due to the small size of endosomes (~500 nm in diameter) and the highly dynamic nature of these domains. Two recent technical innovations have enabled direct, real-time visualization of lipid domains during endosomal escape in live cells. We treated HeLa cells with a phosphatidylinositol-3-phosphate kinase-FYVE inhibitor, which increases endosome diameter from approximately 0.5 μm to ~2 μm.[16] These enlarged endosomes were then imaged in real-time by conventional laser-scanning confocal microscopy. This approach revealed that both CPPs[16] and bacterial toxins (e.g., diphtheria toxin)[17] induced the formation of lipid domains on the endosomal membrane, which subsequently budded out as small vesicles and collapsed.

Wittrup and co-workers leveraged the improved resolution and signal-to-noise ratio of Airyscan confocal microscopy to

https://doi.org/10.1021/acsnano.5c11721
ACS Nano 2025, 19, 40293−40303

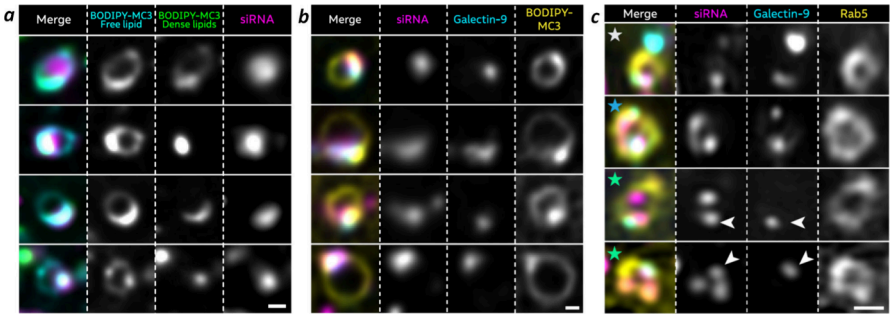

Figure 3. Distribution of MC3, siRNA, galectin-9, and Rab5 with respect to the endosomal membrane. (a) Super-resolution confocal microscopic images of individual endosomes in HeLa cells treated with 100 nM AF647-siRNA BODIPY-MC3 LNPs for 2−4 h and imaged using a VT-iSIM microscope. (b) Similar to (a) but with the galectin-9 signal included. (c) Super-resolution images of Rab5$^+$ endosomes with siRNA-LNP and galectin-9 foci inside, outside, or associated with the membrane. HeLa cells expressing YFP-galectin-9 and mScarlet-Rab5 were incubated with 100 nM AF6471/4-siRNA-LNPs for 90 min, fixed, and imaged using Airyscan confocal microscopy. Scale bars, 500 nm. Adapted from ref 30. Available under a CC-BY 4.0. Copyright 2025 Springer Nature America, Inc.

visualize LNP endosomal escape in live HeLa cells.[30] They designed LNPs incorporating both fluorescently labeled siRNA (AF647) and a BODIPY-labeled DLin-MC3-DMA lipid (BODIPY-MC3). Intact dual-labeled LNPs display significant FRET from BODIPY to AF647, which disappears after LNP disintegration. They found that intact LNPs, exhibiting low BODIPY fluorescence and efficient FRET, were primarily localized in the periphery of cells and rarely in perinuclear regions. In contrast, structures with high BODIPY intensity (disintegrated LNP remnants) were typically present in perinuclear regions. In a subset of Rab5$^+$ endosomal structures, BODIPY-MC3 appeared integrated into the vesicle membrane but was not uniformly distributed throughout (Figure 3a,b). The presence of regions with intense BODIPY fluorescence is consistent with the formation of lipid domains enriched in BODIPY-MC3. In some endosomes, siRNA was homogeneously dispersed in the lumen, while in others, siRNA formed particulate foci generally in close vicinity to the BODIPY-MC3 lipid domains. The simplest explanation is that free siRNA molecules released from disintegrated LNPs were attracted to the positively charged lipid domains through electrostatic interactions. However, the colocalization or recruitment of RNAs to cationic lipid domains was not always effective; some perinuclear vesicles contained either BODIPY$^+$ or AF647$^+$ structures, but not both. This suggests that BODIPY-MC3 and siRNA cargo had separated into different endosomal compartments during endosomal trafficking (presumably due to lateral fusion and fission of the endosomes). VBC events originating from these BODIPY$^+$ but RNA-free vesicles would lead to nonproductive endosomal escape, releasing CILs but not RNA cargo into the cytosol. Indeed, the observed "hit" rate (defined as the fraction of "damaged vesicles" with detectable RNA cargo) ranged from 67% to 74% for siRNA-LNPs but was only ~20% for mRNA-LNPs. The formation of cationic lipid domains and the recruitment of RNA cargo to these domains have also been observed in model systems.[37,40]

Vesicle Budding and Collapse. Over the past decade, mechanistic studies of nucleic acid endosomal escape mediated by polyplexes,[27] lipoplexes,[11,27,29] LNPs,[9−12,30] and small molecules[28] have revealed striking commonalities. Endosomal escape typically results in a sudden and partial release of nucleic acid cargo into the cytosol (i.e., quantal kinetics), followed by the rapid recruitment of galectin-8 and/or -9 to "damaged endosomes," but with a slow release of remaining nucleic acids (Figures 3b, 3c, and 4a). While challenging to reconcile with the

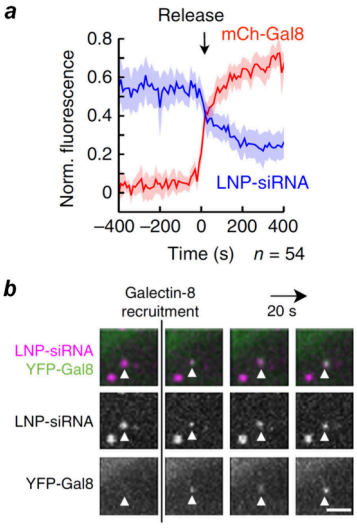

Figure 4. Release of LNP siRNAs from maturing endosomes and recruitment of galectin-8 in HeLa cells. (a) HeLa cells expressing mCherry−galectin-8 (mCh-Gal8) were incubated with LNP−siRNA-AF647 and imaged every 10 s, and fluorescence intensities of vesicles that became mCh-Gal8$^+$ were quantified as a function of time (time of positive mCh-Gal8 signal = 0). Blue line, average normalized LNP−siRNA-AF647 fluorescence; red line, mCh-Gal8 fluorescence. (b) Time-lapse confocal microscopic images of a pair of LNP-containing vesicles, one of which (indicated by white triangles) collapsed and recruited YFP−galectin-8. YFP−galectin-8−expressing HeLa cells were incubated with LNP−siRNA-AF647 and imaged every 20 s. Scale bar, 2 μm. Adapted with permission from ref 11. Copyright 2015 Springer Nature America, Inc.

proton sponge/osmotic lysis or membrane fusion mechanisms, these features are hallmarks of the VBC mechanism. As demonstrated for CPPs[16,18] and bacterial toxins,[17,43] each VBC event simultaneously releases a bolus of translocating biomolecules from the endosome into the cytosol, initially forming an amorphous aggregate of membrane lipids, the translocating biomolecules, and likely certain cellular proteins. Subsequent dissolution of this aggregate liberates the biomolecules into the cytosol for biological function. It is expected that biomolecules (and lipids) exposed on the aggregate's surface would be immediately released into the cytosol, causing a sudden surge in cytoplasmic concentration. In contrast, the liberation of biomolecules within the aggregate's interior would require varying periods, depending on the aggregate's stability.

https://doi.org/10.1021/acsnano.5c11721
ACS Nano 2025, 19, 40293−40303

Galectin-8 and -9 are cytosolic proteins that recognize β-galactosides on the cell surface or within the lumen of endolysosomal compartments.[44] In recent years, galectin-8 and -9 have been commonly used as proxies for identifying endosomes undergoing active endosomal escape.[45−47] It has been hypothesized that endosomal escape damages the endosomal membrane, exposing β-galactosides to the cytoplasmic leaflet and allowing galectin recruitment to the damaged endosomes. How β-galactosides are *instantaneously* transported from the endosomal lumen to the cytoplasmic leaflet was not clear. Since endosomal escape by VBC does not compromise the integrity of the endosomal membrane, we propose two possible scenarios for the formation of galectin-8/-9 puncta, both of which allow the sudden exposure of β-galactosides to the cytosol. The most likely scenario is that the putative "damaged endosomes" are in fact the amorphous aggregates derived from budded and collapsed vesicles. In these aggregates, the loss of membrane structure exposes the β-galactosides to the cytosol. Alternatively, β-galactosides are released from the aggregates and reintegrated into the membrane of a nearby endosome (e.g., the endosome from which the budded vesicle/aggregate originated). Model studies have revealed that CILs derived from disassembled LNPs are rapidly integrated into a nearby lipid bilayer or monolayer (within a second).[40]

The aforementioned studies have provided additional, compelling evidence for the VBC mechanism. The VBC mechanism involves splitting of a vesicle into two, one of which subsequently collapses while the other remains intact. This sequence of events has been captured by time-lapse confocal microscopy in live cells during the endosomal escape of LNPs (Figure 4b),[11] polyplexes (ref 27, Figure 1 and movie 1a), lipoplexes (ref 27, Figure 5), and bacteria.[45] Super-resolution confocal microscopy also revealed nonvesicular structures rich in siRNA and galectin-9 just outside of Rab5$^+$ endosomes during the endosomal escape of siRNA-LNPs (Figure 3b,c). These structures are highly reminiscent of the aggregates resulting from recently budded and collapsed vesicles.

Cargo Release. Accumulating evidence suggests that an additional postendosomal escape step also affects the functional delivery of nucleic acids into the cytosol. Johnston and colleagues prepared mScarlet mRNA-LNPs with three different FDA-approved CILs—SM-102, MC3, and ALC-0315—and compared their total cellular uptake by endocytosis, cytosolic delivery efficiency, and mScarlet protein expression levels.[48] Interestingly, they found only a limited correlation between the amount of mRNA delivered to the cytosol and protein expression. For example, SM-102 and MC3 exhibited similar endosomal escape and cytosolic delivery efficiencies, and yet dramatically different mScarlet expression levels, with SM-102 being ~10-fold more efficacious. Several other reports have also hinted that the overall delivery efficiency of nucleic acids might be limited by their slow liberation from insoluble aggregates.[49−53] However, the precise nature of this rate-limiting step has been elusive.

As previously discussed, we posit that after endosomal escape by VBC, the nucleic acid cargo, the contents of the delivery vehicle (e.g., CILs and cationic polymers), and endosomal lipids/proteins form an insoluble aggregate within the cytosol. For cargo molecules exposed to the aggregate's surface and/or having minimal binding affinity for the aggregate (e.g., dextran[28]), their cytosolic release is rapid and complete. Conversely, nucleic acids can bind to cationic lipids and polymers with high affinity; when buried inside aggregates, they are expected to be slowly (and potentially partially) released. Large nucleic acid-containing aggregates have been observed in live cells after treatment with LNPs (Figure 5),[50] lipoplexes,[29]

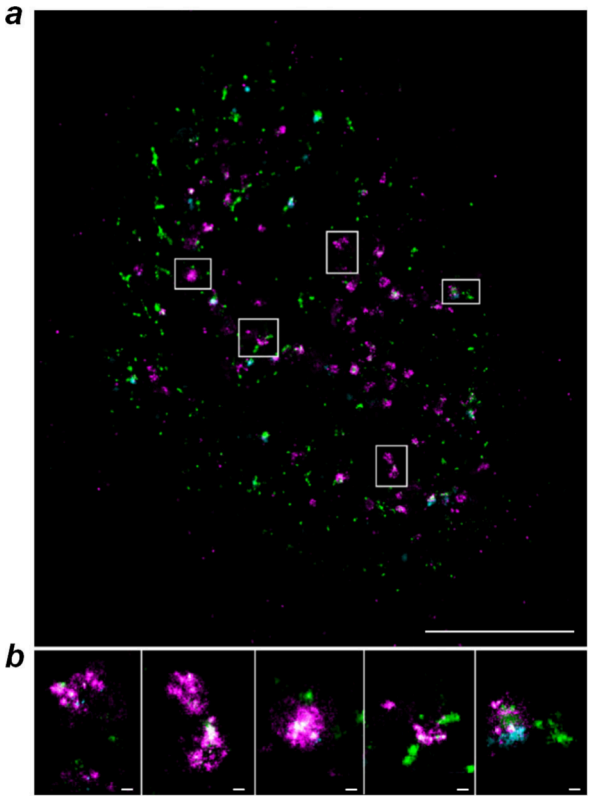

Figure 5. Putative insoluble mRNA/lipid aggregates in HeLa cells treated with MC3 LNP-Cy5-mRNA (magenta), transferrin (green), and EGF (cyan). (a) Super-resolution image of a HeLa cell by multicolor single-molecule localization microscopy (SMLM). Scale bar, 5 μm. (b) Enlarged images for five regions of interest from (a). Scale bar, 100 nm. Reproduced from ref 50. Available under a CC-BY 4.0. Copyright 2021 Rockefeller University Press.

polyplexes,[49] or CPP/mRNA complexes,[52] with some persisting for extended periods (e.g., 24 h). These were likely formed by the conglomeration of smaller aggregates derived from multiple VBC events. This hypothesis provides a plausible explanation for the superior efficacy of SM-102 over MC3 during the functional delivery of mScarlet mRNA: SM-102 contains a branched alkyl chain whereas MC3 does not (Figure 6). The branched structure of SM-102 likely forms less tightly packed post-VBC aggregates, thereby facilitating the liberation of mRNAs from the aggregates. ALC-0315, which also has branched alkyl groups, is ~ 3-fold more efficient in cargo release than MC3.[48] LNPs containing terminally branched CILs appear to be generally more efficacious than their counterparts with linear CILs.[54,55]

RECONCILIATION OF ENIGMATIC LITERATURE OBSERVATIONS

Decades of research and the extensive application of LNPs have generated a body of well-established experimental observations that current mechanistic models cannot fully explain. In the following sections, I apply the VBC mechanism to offer plausible explanations for these observations, thereby providing additional support for the VBC pathway.

https://doi.org/10.1021/acsnano.5c11721
ACS Nano 2025, 19, 40293−40303

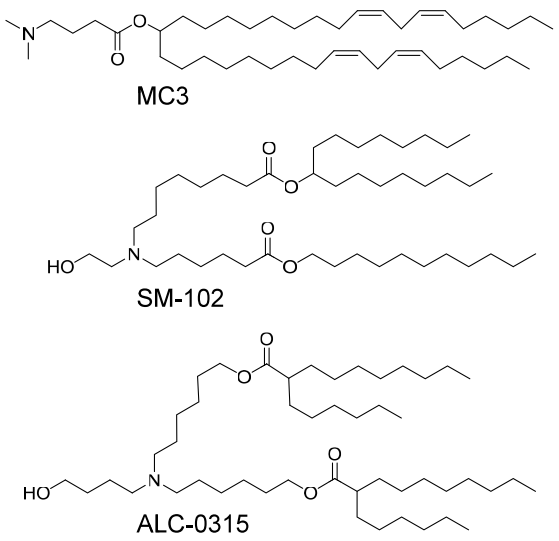

Figure 6. Structures of MC3, SM-102, and ALC-0315.

Poor Delivery Efficiency of Current LNPs. Several studies have reported that for siRNA-LNPs, only 1−3% of endocytosed siRNA reaches the cytosol.[9,11,12] While it was widely assumed that low endosomal escape efficiency was primarily to blame, it is now clear that the situation is more nuanced, with siRNA attrition occurring at multiple stages. Attrition first takes place immediately following endocytic uptake, with as much as 70% of endocytosed siRNA being eventually recycled back to the cell surface.[10] Subsequently, endosomal escape is limited by at least two factors: 1) not all LNP-containing endosomes undergo VBC events, and 2) when they do, only a fraction of the budded vesicles (∼70% for siRNAs and ∼20% for mRNAs) contain the nucleic acid cargo.[11,30] Specifically, disassembly of LNPs, especially those of mRNAs, is incomplete in the early and maturing endosomes, the main compartments of endosomal escape.[30] Incomplete disassembly of LNPs limits the number of free CILs available to drive VBC events. The partially disassembled LNPs may also compete with the lipid domains for binding to the RNA cargo. Both factors decrease the efficiency of endosomal escape. Finally, only a fraction of the nucleic acid cargo is liberated from the post-VBC aggregates,[48] while the remainder appears to be degraded through autophagy or transported out of the cell in extracellular vesicles (EVs).[10−12] The reported endosomal escape efficiencies for three FDA-approved CILs (SM-102, MC3, and ALC-0315) were approximately 10%, 5%, and 4%, respectively.[48] These values are likely somewhat underestimated, as they were based on the amount of a 20-mer oligonucleotide probe available for enzymatic reaction within the cytosol. They did not account for the fraction of molecules that escaped the endosome but remained entrapped within the post-VBC aggregates.

Improved Activity of β-Sitosterol over Cholesterol. The substitution of β-sitosterol for cholesterol has been previously reported to improve the nucleic acid delivery efficiency of LNPs, attributed to more efficient endosomal escape.[56] A recent study confirmed the superior activity of LNPs containing β-sitosterol over those with cholesterol, demonstrating a 4-fold increase in mScarlet expression.[48] However, this improved activity was primarily caused by an ∼2-fold increase in endocytic uptake of the β-sitosterol-containing LNP and, postendosomal escape, an ∼2-fold more efficient mRNA release. Their endosomal escape efficiencies were found to be virtually identical. Both sterols function by interacting with and modulating phospholipid bilayers.[57] While cholesterol's unique structure is ideally suited for efficient and tight packing within the hydrophobic core of the membrane, β-sitosterol possesses an extra ethyl group at C-24. This branched, bulkier side chain prevents it from fitting snugly into the hydrophobic core of the phospholipid bilayer.[57,58] Consequently, a more loosely packed, β-sitosterol-containing post-VBC aggregate is expected to facilitate RNA release, explaining the improved cargo liberation observed.

Correlation between Endosomal Escape Efficiency and Cubic Phase Formation. The ability of CILs to form the inverse hexagonal (H_{II}) phase was previously considered critical for endosomal escape via the membrane fusion/damage mechanism.[14,34,35] However, several recent studies reveal a positive correlation between endosomal escape efficiency and the CIL's ability to form bicontinuous cubic (Q_{II}) phases.[36,51,59] Furthermore, the inclusion of Q_{II} phase-promoting helper lipids also improves the delivery efficiency of LNPs.[60] These phenomena can be readily explained by the VBC mechanism. During a VBC event, the budding neck, characterized by acute membrane curvatures, possesses the highest potential energy, analogous to the transition state of a chemical reaction (Figure 7).[19] These membrane curvatures are often described as

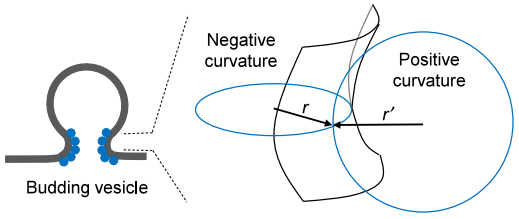

Figure 7. Scheme showing a budding neck enriched with the translocating biomolecules (blue spheres) and the negative Gaussian curvature at the budding neck (with positive and negative curvatures in the vertical and horizontal directions, respectively).

negative Gaussian curvature, featuring simultaneous positive and negative membrane curvatures in orthogonal directions but an overall curvature of approximately zero.[61] Thus, to promote VBC and subsequent endosomal escape, a biomolecule must be capable of simultaneously inducing (and/or accommodating) both positive and negative curvatures in orthogonal directions.[19] Biomolecules effective for promoting negative Gaussian curvature are typically amphipathic molecules, including CPPs,[16,18] viral proteins/peptides,[62] and certain lipids.[63] Significantly, negative Gaussian curvature is a defining feature of Q_{II} phases,[61] providing a direct link between lipid phase behavior and the energetics of VBC.

Endosomal Escape during a "Window of Opportunity". Depending on the delivery modality, endosomal escape may occur from different compartments along the endolysosomal pathway, but typically during a narrow "window of opportunity".[6] Thus, polyplexes are released from late endosomes,[27] while chloroquine-mediated siRNA release was from late endosomes and lysosomes.[28] For LNPs, most of the studies have demonstrated RNA release from early, maturing, and/or recycling endosomes,[9,11,30,50] although release from late endosomes has also been reported.[10] The VBC mechanism offers a potential explanation for this narrow "window of opportunity". Neutral CILs, such as SM-102, ALC-0315, and MC3, are inverse cone-shaped molecules that possess strong negative intrinsic

https://doi.org/10.1021/acsnano.5c11721
ACS Nano 2025, 19, 40293−40303

curvature and form inverse micellar and H_{II} structures. Protonation of the CILs increases their headgroup sizes within a membrane due to electrostatic repulsion and increased hydration. Their *partial* protonation—occurring in the mildly acidic environment of early, maturing, and recycling endosomes (pH 6.0–6.5)—moderates their negative intrinsic curvature, while endowing them the ability to recruit RNA cargo. Lipids of intermediate negative intrinsic curvatures facilitate the formation of negative Gaussian curvature and the budding neck required for VBC.[59,64] Conversely, further protonation in the more acidic late endosomes and lysosomes (pH 4.5–5.5) promotes the formation of lamellar phases,[59,64] thereby inhibiting the VBC process. For different delivery modalities or LNPs of different compositions, the optimal pH for VBC is likely to be different.

CONCLUSION AND FUTURE DIRECTIONS

The most significant bottleneck in nucleic acid delivery by LNPs remains efficient endosomal escape. In this perspective, I have marshaled literature evidence to position the VBC mechanism as the critical pathway for LNP endosomal escape. The VBC model is supported by particularly compelling evidence from recent live-cell studies—such as the elegant work[30] demonstrating LNP disassembly, CIL domain formation, and colocalization with RNA during escape—which cannot be fully explained by prior models. The VBC mechanism differs from the older models in key aspects: topological (VBC) vs physical translocation (pore formation), partial and sudden release (VBC) vs complete release of cargo (fusion and lysis), and membrane integrity (VBC) vs catastrophic rupture of the endosomal membrane (lysis). This model is fully consistent with the broad body of LNP literature and highlights a postescape challenge: the dissolution of post-VBC aggregates as an additional kinetic bottleneck for functional nucleic acid delivery. Thus, the VBC mechanism is not a superficial variation but a distinct and superior mechanistic model that changes our understanding of LNP function. Nevertheless, to move the VBC mechanism from a theoretical framework to a fully validated mechanism, acquiring more direct, real-time evidence remains the essential and urgent goal for advancing the field of LNP engineering.

Direct Experimental Validation of VBC Intermediates. The immediate future direction must focus on directly observing the VBC process *in situ*. A potential approach may involve dual labeling of LNPs and the cell membrane with fluorescent dyes and monitoring endosomal trafficking in live cells and real-time by confocal microscopy, as previously described for CPPs[16] and bacterial toxins.[17] Briefly, one may label the CIL or RNA cargo with pHAb, a pH-sensitive dye with strong red fluorescence at pH $\leq$ 6 but essentially nonfluorescent at neutral or basic pH, and the cell membrane with a green dye (pH-insensitive). During VBC from the endosomal membrane, a freshly budded vesicle would fluoresce in both green and red channels, while collapse of the vesicle would result in the sudden loss of red (but not green) fluorescence. The fluorescence intensity of the budded vesicle, relative to that of the remaining endosome, would provide a quantitative assessment of the endosomal escape efficiency. Alternatively, one may employ super-resolution microscopy (e.g., Airyscan confocal microscopy[30]) to directly visualize the various VBC intermediates and potentially entire VBC events.

Unraveling the Molecular Underpinnings. An unresolved, key question is what drives the collapse of budded vesicles and the molecular underpinning of the collapse event. Because of the small size and transient nature of the budded vesicles (i.e., they typically collapse within a few seconds postbudding), experimental characterization of the budded vesicles has not been possible; computational approaches may thus provide critical insight into this key step. Another key question is whether cellular proteins are involved in the VBC/endosomal escape process. While the minimal VBC mechanism is energy-independent and can occur on model membranes without any protein,[15] host factors like SNAREs, ESCRT complexes, or GTPases are likely to modulate the VBC process in a living cell. Identifying and characterizing these proteins represent an important direction of future research. Last but not least, robust assay methods need to be developed to quantitate the efficiency and kinetics of the two postuptake bottlenecks: VBC/endosomal escape and the dissolution of post-VBC aggregates.

Design Strategies to Exploit the VBC Mechanism. While further research is essential to fully elucidate the molecular details of VBC, this mechanism offers critical and immediate insights for the future design of improved LNPs. Based on these insights, I propose the following strategies to enhance the overall delivery efficiency of LNPs:

Optimized Endocytic Uptake. As demonstrated by Johnston and co-workers, LNPs differing only in their CIL (e.g., SM-102 vs ALC-0315) exhibit vastly different cellular uptake efficiencies.[48] Similarly, the substitution of β-sitosterol for cholesterol significantly increased endocytic uptake (~2-fold).[48,56] These observations highlight considerable opportunities to enhance LNP endocytic uptake through strategic modifications to CILs, helper lipids, and/or cholesterol components.

Reduced LNP Recycling. While small molecule inhibitors of the recycling pathway have been explored,[65,66] their potential for cellular and systemic toxicity warrants caution. Future research should investigate whether structural modifications to the LNP itself can effectively reduce the amount of LNP recycling, thereby retaining more cargo within the endosomal pathway.

Enhanced Endosomal Escape Efficiency. This area likely represents the greatest opportunity for improvement, given the currently low endosomal escape efficiencies of LNPs. One promising approach involves designing CILs, helper lipids, and/or cholesterol analogs that permit more efficient disassembly of LNPs in the early/maturing endosome and more effectively induce negative Gaussian curvature in a pH-responsive manner. Specifically, the lipids should generate an overall membrane curvature of ~0 in early/maturing endosomes. It will be of particular interest to determine whether the inclusion of a proper amount of lipids with positive intrinsic curvature (e.g., lysophospholipids) into LNPs could facilitate VBC and endosomal escape. Furthermore, improving the colocalization of the nucleic acid cargo with CIL domains should increase the "hit rate" of productive endosomal escape events. Another strategy may involve covalently conjugating or encapsulating molecules known to promote endosomal escape, such as amphipathic CPPs[67] or phospholipases,[19,68] to/into LNPs.

Increased Cargo Release from Post-VBC Aggregates. This postendosomal escape step remains underexplored but is likely of particular importance for large cargos like mRNAs. This challenge may be addressed by modifying LNP components, the nucleic acid cargo, or both, with the objective of forming less tightly packed aggregates after VBC events, thus facilitating more complete and rapid cargo liberation into the cytosol.

https://doi.org/10.1021/acsnano.5c11721
ACS Nano 2025, 19, 40293–40303

AUTHOR INFORMATION

Corresponding Author

Dehua Pei − *Department of Chemistry and Biochemistry, The Ohio State University, Columbus, Ohio 43210, United States;* orcid.org/0000-0002-2057-6934; Email: pei.3@osu.edu

Complete contact information is available at: https://pubs.acs.org/10.1021/acsnano.5c11721

Funding

This work was supported by the National Institutes of Health (GM122459).

Notes

The author declares no competing financial interest.

An earlier version of this manuscript has been deposited as a preprint: Pei, D. Endosomal Escape of Lipid Nanoparticles: A New Perspective on the Literature Data, July 16, 2025 Version 1. *ChemRxiv*. DOI: 10.26434/chemrxiv-2025-t8115.

ACKNOWLEDGMENTS

I thank Prabhat Bhat of the Pei Group for assistance with the artwork in Figure 2.

ABBREVIATIONS

CIL, cationic ionizable lipid; CPP, cell-penetrating peptide; LNP, lipid nanoparticle; mRNA, mRNA; siRNA, small interfering RNA; VBC, vesicle budding and collapse.

REFERENCES

(1) Witten, J.; Hu, Y.; Langer, R.; Anderson, D. G. Recent Advances in Nanoparticulate RNA Delivery Systems. *Proc. Natl. Acad. Sci. U. S. A.* **2024**, *121*, No. e2307798120.

(2) Hou, X.; Zaks, T.; Langer, R.; Dong, Y. Lipid Nanoparticles for mRNA Delivery. *Nat. Rev. Mater.* **2021**, *6*, 1078−1094.

(3) Akinc, A.; Maier, M. A.; Manoharan, M.; Fitzgerald, K.; Jayaraman, M.; Barros, S.; Ansell, S.; Du, X.; Hope, M. J.; Madden, T. D.; Mui, B. L.; Semple, S. C.; Tam, Y. K.; Ciufolini, M.; Witzigmann, D.; Kulkarni, J. A.; van der Meel, R.; Cullis, P. R. The Onpattro Story and the Clinical Translation of Nanomedicines Containing Nucleic Acid-Based Drugs. *Nat. Nanotechnol.* **2019**, *14*, 1084−1087.

(4) Baden, L. R.; El Sahly, H. M.; Essink, B.; Kotloff, K.; Frey, S.; Novak, R.; Diemert, D.; Spector, S. A.; Rouphael, N.; Creech, C. B.; McGettigan, J.; Khetan, S.; Segall, N.; Solis, J.; Brosz, A.; Fierro, C.; Schwartz, H.; Neuzil, K.; Corey, L.; Gilbert, P. COVE Study Group. Efficacy and Safety of the mRNA-1273 SARS-CoV-2 Vaccine. *N. Engl. J. Med.* **2021**, *384*, 403−416.

(5) Simonsen, J. B. Lipid Nanoparticle-Based Strategies for Extrahepatic Delivery of Nucleic Acid Therapies - Challenges and Opportunities. *J. Controlled Release* **2024**, *370*, 763−772.

(6) Chatterjee, S.; Kon, E.; Sharma, P.; Peer, D. Endosomal Escape: A Bottleneck for LNP-Mediated Therapeutics. *Proc. Natl. Acad. Sci. U. S. A.* **2024**, *121*, No. e2307800120.

(7) Dowdy, S. F.; Setten, R. L.; Cui, X. S.; Jadhav, S. G. Delivery of RNA Therapeutics: The Great Endosomal Escape! *Nucl. Acid Ther.* **2022**, *32*, 361−368.

(8) Escalona-Rayo, O.; Papadopoulou, P.; Slütter, B.; Kros, A. Biological Recognition and Cellular Trafficking of Targeted RNA-lipid Nanoparticles. *Curr. Opin. Biotechnol.* **2024**, *85*, No. 103041.

(9) Gilleron, J.; Querbes, W.; Zeigerer, A.; Borodovsky, A.; Marsico, G.; Schubert, U.; Manygoats, K.; Seifert, S.; Andree, C.; Stöter, M.; Epstein-Barash, L.; Zhang, L.; Koteliansky, V.; Fitzgerald, K.; Fava, E.; Bickle, M.; Kalaidzidis, Y.; Akinc, A.; Maier, M.; Zerial, M. Image-Based Analysis of Lipid Nanoparticle-Mediated siRNA Delivery, Intracellular Trafficking and Endosomal Escape. *Nat. Biotechnol.* **2013**, *31*, 638−646.

(10) Sahay, G.; Querbes, W.; Alabi, C.; Eltoukhy, A.; Sarkar, S.; Zurenko, C.; Karagiannis, E.; Love, K.; Chen, D.; Zoncu, R.; Buganim, Y.; Schroeder, A.; Langer, R.; Anderson, D. G. Efficiency of siRNA Delivery by Lipid Nanoparticles Is Limited by Endocytic Recycling. *Nat. Biotechnol.* **2013**, *31*, 653−658.

(11) Wittrup, A.; Ai, A.; Liu, X.; Hamar, P.; Trifonova, R.; Charisse, K.; Manoharan, M.; Kirchhausen, T.; Lieberman, J. Visualizing Lipid-Formulated siRNA Release from Endosomes and Target Gene Knockdown. *Nat. Biotechnol.* **2015**, *33*, 870−876.

(12) Maugeri, M.; Nawaz, M.; Papadimitriou, A.; Angerfors, A.; Camponeschi, A.; Na, M.; Hölttä, M.; Skantze, P.; Johansson, S.; Sundqvist, M.; Lindquist, J.; Kjellman, T.; Mårtensson, I.-L.; Jin, T.; Sunnerhagen, P.; Östman, S.; Lindfors, L.; Valadi, H. Linkage between Endosomal Escape of LNP-mRNA and Loading into EVs for Transport to Other Cells. *Nat. Commun.* **2019**, *10*, No. 4333.

(13) Behr, J.-P. The Proton Sponge: A Trick to Enter Cells the Viruses Did Not Exploit. *CHIMIA Int. J. Chem.* **1997**, *51*, 34−36.

(14) Semple, S. C.; Akinc, A.; Chen, J.; Sandhu, A. P.; Mui, B. L.; Cho, C. K.; Sah, D. W.; Stebbing, D.; Crosley, E. J.; Yaworski, E.; Hafez, I. M.; Dorkin, J. R.; Qin, J.; Lam, K.; Rajeev, K. G.; Wong, K. F.; Jeffs, L. B.; Nechev, L.; Eisenhardt, M. L.; Jayaraman, M.; Kazem, M.; Maier, M. A.; Srinivasulu, M.; Weinstein, M. J.; Chen, Q.; Alvarez, R.; Barros, S. A.; De, S.; Klimuk, S. K.; Borland, T.; Kosovrasti, V.; Cantley, W. L.; Tam, Y. K.; Manoharan, M.; Ciufolini, M. A.; Tracy, M. A.; de Fougerolles, A.; MacLachlan, I.; Cullis, P. R.; Madden, T. D.; Hope, M. J. Rational Design of Cationic Lipids for siRNA Delivery. *Nat. Biotechnol.* **2010**, *28*, 172−176.

(15) Qian, Z.; Martyna, A.; Hard, R. L.; Wang, J.; Appiah-Kubi, G.; Coss, C.; Phelps, M. A.; Rossman, J. S.; Pei, D. Discovery and Mechanism of Highly Efficient Cyclic Cell-penetrating Peptides. *Biochemistry* **2016**, *55*, 2601−2612.

(16) Sahni, A.; Qian, Z.; Pei, D. Cell-Penetrating Peptides Escape the Endosome by Inducing Vesicle Budding and Collapse. *ACS Chem. Biol.* **2020**, *15*, 2485−2492.

(17) Sahni, A.; Pei, D. Bacterial Toxins Escape the Endosome by Inducing Vesicle Budding and Collapse. *ACS Chem. Biol.* **2021**, *16*, 2415−2422.

(18) Sahni, A.; Ritchey, J. L.; Qian, Z.; Pei, D. Cell-Penetrating Peptides Translocate across the Plasma Membrane by Inducing Vesicle Budding and Collapse. *J. Am. Chem. Soc.* **2024**, *146*, 25371−25382.

(19) Pei, D. How Do Biomolecules Cross the Cell Membrane? *Acc. Chem. Res.* **2022**, *55*, 309−318.

(20) Pei, D.; Dalbey, R. E. Membrane Translocation of Folded Proteins. *J. Biol. Chem.* **2022**, *298*, No. 102107.

(21) Huff, J. The Airyscan detector from ZEISS: confocal imaging with improved signal-to-noise ratio and super-resolution. *Nat. Methods* **2015**, *12*, i−ii.

(22) Nakano, A. Spinning-Disk Confocal Microscopy: A Cutting-Edge Tool for Imaging Membrane Traffic. *Cell Struct. Funct.* **2002**, *27*, 349−355.

(23) Akinc, A.; Thomas, M.; Klibanov, A. M.; Langer, R. Exploring Polyethylenimine-mediated DNA Transfection and the Proton Sponge Hypothesis. *J. Gene Med.* **2005**, *7*, 657−663.

(24) Li, Z.; Carter, J.; Santos, L.; Webster, C.; van der Walle, C. F.; Li, P.; Rogers, S. E.; Lu, J. R. Acidification-Induced Structure Evolution of Lipid Nanoparticles Correlates with Their *In Vitro* Gene Transfections. *ACS Nano* **2023**, *17*, 979−990.

(25) Akinc, A.; Zumbuehl, A.; Goldberg, M.; Leshchiner, E. S.; Busini, V.; Hossain, N.; Bacallado, S. A.; Nguyen, D. N.; Fuller, J.; Alvarez, R.; Borodovsky, A.; Borland, T.; Constien, R.; de Fougerolles, A.; Dorkin, J. R.; Narayanannair Jayaprakash, K.; Jayaraman, M.; John, M.; Koteliansky, V.; Manoharan, M.; Nechev, L.; Qin, J.; Racie, T.; Raitcheva, D.; Rajeev, K. G.; Sah, D. W.; Soutschek, J.; Toudjarska, I.; Vornlocher, H. P.; Zimmermann, T. S.; Langer, R.; Anderson, D. G. A Combinatorial Library of Lipid-Like Materials for Delivery of RNAi Therapeutics. *Nat. Biotechnol.* **2008**, *26*, 561−569.

(26) Jayaraman, M.; Ansell, S. M.; Mui, B. L.; Tam, Y. K.; Chen, J.; Du, X.; Butler, D.; Eltepu, L.; Matsuda, S.; Narayanannair, J. K.; Rajeev, K. G.; Hafez, I. M.; Akinc, A.; Maier, M. A.; Tracy, M. A.; Cullis, P. R.; Madden, T. D.; Manoharan, M.; Hope, M. J. Maximizing the Potency of

Lipid Nanoparticle Formulations for siRNA Delivery to the Liver. *Angew. Chem., Int. Ed.* **2012**, *51*, 8529−8533.
(27) ur Rehman, Z.; Hoekstra, D.; Zuhorn, I. S. Mechanism of Polyplex- And Lipoplex-Mediated Delivery of Nucleic Acids: Real-Time Visualization of Transient Membrane Destabilization Without Endosomal Lysis. *ACS Nano* **2013**, *7*, 3767−3777.
(28) Du Rietz, H.; Hedlund, H.; Wilhelmson, S.; Nordenfelt, P.; Wittrup, A. Imaging Small Molecule-Induced Endosomal Escape of siRNA. *Nat. Commun.* **2020**, *11*, No. 1809.
(29) Hedlund, H.; Du Rietz, H.; Johansson, J. M.; Eriksson, H. C.; Zedan, W.; Huang, L.; Wallin, J.; Wittrup, A. Single-Cell Quantification and Dose-Response of Cytosolic siRNA Delivery. *Nat. Commun.* **2023**, *14*, No. 1075.
(30) Johansson, J. M.; Du Rietz, H.; Hedlund, H.; Eriksson, H. C.; Oude Blenke, E.; Pote, A.; Harun, S.; Nordenfelt, P.; Lindfors, L.; Wittrup, A. Cellular and Biophysical Barriers to Lipid Nanoparticle Mediated Delivery of RNA to the Cytosol. *Nat. Commun.* **2025**, *16*, No. 5354.
(31) Białas, N.; Müller, E. K.; Epple, M.; Hilger, I. Silica-coated Calcium Phosphate Nanoparticles for Gene Silencing of NF-kB P65 by siRNA and Their Impact on Cellular Players of Inflammation. *Biomaterials* **2021**, *276*, No. 121013.
(32) Mishra, S.; Webster, P.; Davis, M. E. PEGylation Significantly Affects Cellular Uptake and Intracellular Trafficking of Non-Viral Gene Delivery Particles. *Eur. J. Cell Biol.* **2004**, *83*, 97−111.
(33) Hatakeyama, H.; Akita, H.; Harashima, H. The Polyethyleneglycol Dilemma: Advantage and Disadvantage of PEGylation of Liposomes for Systemic Genes and Nucleic Acids Delivery to Tumors. *Biol. Pharm. Bull.* **2013**, *36*, 892−899.
(34) Hafez, I. M.; Maurer, N.; Cullis, P. R. On the Mechanism Whereby Cationic Lipids Promote Intracellular Delivery of Polynucleic Acids. *Gene Ther.* **2001**, *8*, 1188−1196.
(35) Heyes, J.; Palmer, L.; Bremner, K.; MacLachlan, I. Cationic Lipid Saturation Influences Intracellular Delivery of Encapsulated Nucleic Acids. *J. Controlled Release* **2005**, *107*, 276−287.
(36) Zheng, L.; Bandara, S. R.; Tan, Z.; Leal, C. Lipid Nanoparticle Topology Regulates Endosomal Escape and Delivery of RNA to the Cytoplasm. *Proc. Natl. Acad. Sci. U. S. A.* **2023**, *120*, No. e2301067120.
(37) Rosenblum, D.; Gutkin, A.; Kedmi, R.; Ramishetti, S.; Veiga, N.; Jacobi, A. M.; Schubert, M. S.; Friedmann-Morvinski, D.; Cohen, Z. R.; Behlke, M. A.; Lieberman, J.; Peer, D. CRISPR-Cas9 Genome Editing Using Targeted Lipid Nanoparticles for Cancer Therapy. *Sci. Adv.* **2020**, *6*, No. eabc9450.
(38) Spadea, A.; Jackman, M.; Cui, L.; Pereira, S.; Lawrence, M. J.; Campbell, R. A.; Ashford, M. Nucleic Acid-Loaded Lipid Nanoparticle Interactions with Model Endosomal Membranes. *ACS Appl. Mater. Interfaces* **2022**, *14*, 30371−30384.
(39) Aliakbarinodehi, N.; Gallud, A.; Mapar, M.; Wesén, E.; Heydari, S.; Jing, Y.; Emilsson, G.; Liu, K.; Sabirsh, A.; Zhdanov, V. P.; Lindfors, L.; Esbjörner, E. K.; Höök, F. Interaction Kinetics of Individual mRNA-Containing Lipid Nanoparticles with an Endosomal Membrane Mimic: Dependence on pH, Protein Corona Formation, and Lipoprotein Depletion. *ACS Nano* **2022**, *16*, 20163−20173.
(40) Aliakbarinodehi, N.; Niederkofler, S.; Emilsson, G.; Parkkila, P.; Olsén, E.; Jing, Y.; Sjöberg, M.; Agnarsson, B.; Lindfors, L.; Höök, F. Time-Resolved Inspection of Ionizable Lipid-Facilitated Lipid Nanoparticle Disintegration and Cargo Release at an Early Endosomal Membrane Mimic. *ACS Nano* **2024**, *18*, 22989−23000.
(41) Duchardt, F.; Fotin-Mleczek, M.; Schwarz, H.; Fischer, R.; Brock, R. A Comprehensive Model for the Cellular Uptake of Cationic Cell-Penetrating Peptides. *Traffic* **2007**, *8*, 848−866.
(42) Hirose, H.; Takeuchi, T.; Osakada, H.; Pujals, S.; Katayama, S.; Nakase, I.; Kobayashi, S.; Haraguchi, T.; Futaki, S. Transient Focal Membrane Deformation Induced by Arginine-Rich Peptides Leads to Their Direct Penetration into Cells. *Mol. Ther.* **2012**, *20*, 984−993.
(43) Hudson, T. H.; Neville, D. M., Jr. Quantal Entry of Diphtheria Toxin to the Cytosol. *J. Biol. Chem.* **1985**, *260*, 2675−2680.
(44) Yang, R. Y.; Rabinovich, G. A.; Liu, F. T. Galectins: Structure, Function and Therapeutic Potential. *Expert Rev. Mol. Med.* **2008**, *10*, No. e17.
(45) Thurston, T. L.; Wandel, M. P.; von Muhlinen, N.; Foeglein, A.; Randow, F. Galectin 8 Targets Damaged Vesicles for Autophagy to Defend Cells against Bacterial Invasion. *Nature* **2012**, *482*, 414−418.
(46) Kilchrist, K. V.; Dimobi, S. C.; Jackson, M. A.; Evans, B. C.; Werfel, T. A.; Dailing, E. A.; Bedingfield, S. K.; Kelly, I. B.; Duvall, C. L. Gal8 Visualization of Endosome Disruption Predicts Carrier-Mediated Biologic Drug Intracellular Bioavailability. *ACS Nano* **2019**, *13*, 1136−1152.
(47) Munson, M. J.; O'Driscoll, G.; Silva, A. M.; Lázaro-Ibáñez, E.; Gallud, A.; Wilson, J. T.; Collén, A.; Esbjörner, E. K.; Sabirsh, A. A High-Throughput Galectin-9 Imaging Assay for Quantifying Nanoparticle Uptake, Endosomal Escape and Functional RNA Delivery. *Commun. Biol.* **2021**, *4*, No. 211.
(48) Liu, H.; Chen, M. Z.; Payne, T.; Porter, C. J. H.; Pouton, C. W.; Johnston, A. P. R. Beyond the Endosomal Bottleneck: Understanding the Efficiency of mRNA/LNP Delivery. *Adv. Funct. Mater.* **2024**, *34*, No. 2404510.
(49) Wojnilowicz, M.; Glab, A.; Bertucci, A.; Caruso, F.; Cavalieri, F. Super-resolution Imaging of Proton Sponge-Triggered Rupture of Endosomes and Cytosolic Release of Small Interfering RNA. *ACS Nano* **2019**, *13*, 187−202.
(50) Paramasivam, P.; Franke, C.; Stöter, M.; Höijer, A.; Bartesaghi, S.; Sabirsh, A.; Lindfors, L.; Arteta, M. Y.; Dahlén, A.; Bak, A.; Andersson, S.; Kalaidzidis, Y.; Bickle, M.; Zerial, M. Endosomal Escape of Delivered mRNA from Endosomal Recycling Tubules Visualized at the Nanoscale. *J. Cell Biol.* **2022**, *221*, No. e202110137.
(51) Philipp, J.; Dabkowska, A.; Reiser, A.; Frank, K.; Krzysztoń, R.; Brummer, C.; Nickel, B.; Blanchet, C. E.; Sudarsan, A.; Ibrahim, M.; Johansson, S.; Skantze, P.; Skantze, U.; Östman, S.; Johansson, M.; Henderson, N.; Elvevold, K.; Smedsrød, B.; Schwierz, N.; Lindfors, L.; Rädler, J. O. pH-Dependent Structural Transitions in Cationic Ionizable Lipid Mesophases Are Critical for Lipid Nanoparticle Function. *Proc. Natl. Acad. Sci. U. S. A.* **2023**, *120*, No. e2310491120.
(52) Oude Egberink, R.; van Schie, D. M.; Joosten, B.; de Muynck, L. T. A.; Jacobs, W.; van Oostrum, J.; Brock, R. Unraveling mRNA Delivery Bottlenecks of Ineffective Delivery Vectors by Co-Transfection with Effective Carriers. *Eur. J. Pharm. Biopharm.* **2024**, *202*, No. 114414.
(53) Cheung, T. H.; Shoichet, M. S. The Interplay of Endosomal Escape and RNA Release from Polymeric Nanoparticles. *Langmuir* **2025**, *41*, 7174−7190.
(54) Hajj, K. A.; Melamed, J. R.; Chaudhary, N.; Lamson, N. G.; Ball, R. L.; Yerneni, S. S.; Whitehead, K. A. A Potent Branched-Tail Lipid Nanoparticle Enables Multiplexed mRNA Delivery and Gene Editing In Vivo. *Nano Lett.* **2020**, *20*, 5167−5175.
(55) Padilla, M. S.; Mrksich, K.; Wang, Y.; Haley, R. M.; Li, J. J.; Han, E. L.; El-Mayta, R.; Kim, E. H.; Dias, S.; Gong, N.; Teerdhala, S. V.; Han, X.; Chowdhary, V.; Xue, L.; Siddiqui, Z.; Yamagata, H. M.; Kim, D.; Yoon, I. C.; Wilson, J. M.; Radhakrishnan, R.; Mitchell, M. J. Branched Endosomal Disruptor (BEND) Lipids Mediate Delivery of mRNA and CRISPR-Cas9 Ribonucleoprotein Complex for Hepatic Gene Editing and T Cell Engineering. *Nat. Commun.* **2025**, *16*, No. 996.
(56) Patel, S.; Ashwanikumar, N.; Robinson, E.; Xia, Y.; Mihai, C.; Griffith, J. P.; Hou, S.; Esposito, A. A.; Ketova, T.; Welsher, K.; Joyal, J. L.; Almarsson, Ö.; Sahay, G. Naturally-occurring Cholesterol Analogues in Lipid Nanoparticles Induce Polymorphic Shape and Enhance Intracellular Delivery of mRNA. *Nat. Commun.* **2020**, *11*, No. 983.
(57) Dufourc, E. J. Sterols and Membrane Dynamics. *J. Chem. Biol.* **2008**, *1*, 63−77.
(58) Lopez, S.; Bermudez, B.; Montserrat-de la Paz, S.; Jaramillo, S.; Varela, L. M.; Ortega-Gomez, A.; Abia, R.; Muriana, F. J. Membrane Composition and Dynamics: A Target of Bioactive Virgin Olive Oil Constituents. *Biochim. Biophys. Acta* **2014**, *1838*, 1638−1656.
(59) Yu, H.; Iscaro, J.; Dyett, B.; Zhang, Y.; Seibt, S.; Martinez, N.; White, J.; Drummond, C. J.; Bozinovski, S.; Zhai, J. Inverse Cubic and

Hexagonal Mesophase Evolution within Ionizable Lipid Nanoparticles Correlates with mRNA Transfection in Macrophages. *J. Am. Chem. Soc.* **2023**, *145*, 24765−24774.
(60) Iwakawa, K.; Sato, R.; Konaka, M.; Yamada, Y.; Harashima, H.; Sato, Y. Cubic Phase-Inducible Zwitterionic Phospholipids Improve the Functional Delivery of mRNA. *Adv. Sci.* **2025**, *12*, No. e2413016.
(61) McMahon, H. T.; Gallop, J. L. Membrane Curvature and Mechanisms of Dynamic Cell Membrane Remodelling. *Nature* **2005**, *438*, 590−596.
(62) Maier, O.; Galan, D. L.; Wodrich, H.; Wiethoff, C. M. An N-Terminal Domain of Adenovirus Protein VI Fragments Membranes by Inducing Positive Membrane Curvature. *Virology* **2010**, *402*, 11−19.
(63) Tyler, A. I. I.; Barriga, H. M. G.; Parsons, E. S.; McCarthy, N. L. C.; Ces, O.; Law, R. V.; Seddon, J. M.; Brooks, N. J. Electrostatic Swelling of Bicontinuous Cubic Lipid Phases. *Soft Matter* **2015**, *11* (16), 3279−3286.
(64) Seddon, J. M. Inverse Bicontinuous and Discontinuous Phases of Lipids, and Membrane Curvature. *Cells* **2025**, *14*, 716.
(65) Shin, J.; Douglas, C. J.; Zhang, S.; Seath, C. P.; Bao, H. Targeting Recycling Endosomes to Potentiate mRNA Lipid Nanoparticles. *Nano Lett.* **2024**, *24*, 5104−5109.
(66) Finicle, B. T.; Eckenstein, K. H.; Revenko, A. S.; Anderson, B. A.; Wan, W. B.; McCracken, A. N.; Gil, D.; Fruman, D. A.; Hanessian, S.; Seth, P. P.; Edinger, A. L. Simultaneous Inhibition of Endocytic Recycling and Lysosomal Fusion Sensitizes Cells and Tissues to Oligonucleotide Therapeutics. *Nucleic Acids Res.* **2023**, *51*, 1583−1599.
(67) Aschmann, D.; Knol, R. A.; Kros, A. Lipid-Based Nanoparticle Functionalization with Coiled-Coil Peptides for *In Vitro* and *In Vivo* Drug Delivery. *Acc. Chem. Res.* **2024**, *57*, 1098−1110.
(68) Le, H. T.; Rao, G. A.; Hirko, A. C.; Hughes, J. A. Polymeric Nanoparticles Containing Conjugated Phospholipase A2 for Nonviral Gene Delivery. *Mol. Pharmaceutics* **2010**, *7*, 1090−1097.

https://doi.org/10.1021/acsnano.5c11721
ACS Nano 2025, 19, 40293−40303